Parallel Electromagnetically Induced Transparency near Ground-State Cooling of a Trapped-Ion Crystal

Jie Zhang,[1,2,3,‡] Man-Chao Zhang,[1,2,3,‡] Yi Xie,[1,2,3] Chun-Wang Wu,[1,2,3] Bao-Quan Ou,[1,2,3] Ting Chen,[1,2,3] Wan-Su Bao,[4] Paul Haljan,[5] Wei Wu,[1,2,3] Shuo Zhang,[4,*] and Ping-Xing Chen[1,2,3,†]

[1] *Department of Physics, College of Liberal Arts and Sciences, National University of Defense Technology, Changsha, Hunan 410073, China*

[2] *Interdisciplinary Center for Quantum Information, National University of Defense Technology, Changsha, Hunan 410073, China*

[3] *Hunan Key Laboratory of Quantum Information Mechanism and Technology, National University of Defense Technology, Changsha, Hunan 410073, China*

[4] *Henan Key Laboratory of Quantum Information and Cryptography, Zhengzhou Information Science and Technology Institute, Zhengzhou 450001, China*

[5] *Department of Physics, Simon Fraser University, Burnaby, British Columbia V5A 1S6, Canada*

(Received 2 December 2021; revised 13 May 2022; accepted 17 May 2022; published 11 July 2022)

We theoretically propose and experimentally demonstrate a parallel electromagnetically induced transparency (parallel EIT) cooling technique for ion crystals in the Paul trap. It breaks the stringent cooling requirements of the standard EIT cooling, thus allowing, in principle, to simultaneously cool the motional mode spectrum with an arbitrary range. Experimentally a large cooling range over 5 MHz is proved by using a single trapped $^{40}Ca^{+}$ ion. We also observe simultaneous near-ground-state cooling for all motional modes of a 4-ion chain with the best average phonon number of about 0.2. For cooling a large number of modes, we only need to modulate the probe beam of the standard EIT cooling with several rf frequencies. This cooling scheme has no selectivity for the types of ions (e.g., $^{171}Yb^{+}$, $^{40}Ca^{+}$), therefore it would be a powerful tool for initialization of all kinds of operational trapped-ion quantum computers or simulators.

DOI: 10.1103/PhysRevApplied.18.014022

I. INTRODUCTION

Cooling the motional degree of freedom to the ground state is an essential step for manipulating cold atoms (ions) [1–7] and commercial trapped-ion quantum computers [8–10], for which the ground-state cooled motional mode acts as the bus for establishing the quantum entanglement between qubits. In particular, high-fidelity quantum operations [11–14] of ion qubits require cooling the motional modes to the Lamb-Dicke (LD) regime, in which the vibrational amplitude of each ion is much less than the optical wavelength. With increasing size of trapped-ion crystals, cooling a large number of motional modes in one process to near ground state is required to reduce the heating effects from the environment [15,16] and the mutual mode coupling [15,17]. Particularly, the operational fidelity of large-scale quantum computers using transverse mode benefits from the sufficiently cooled axial mode [18]. Therefore, it is necessary to exploit an efficient cooling with high bandwidth to bring all motional modes down to near ground state.

A typical quantum-information processsing with trapped ions starts with cooling, which begins with Doppler cooling [19–22], followed by a ground-state cooling technique, including Sisyphus cooling [23,24], resolved sideband cooling [25–27], and electromagnetically induced transparency (EIT) cooling [28–37]. While Sisyphus cooling is efficient for simultaneous cooling of all motional modes, its cooling limit is not low enough for ground-state preparation [23,24] and it suffers from low cooling rate for hyperfine qubits [24]. Resolved sideband cooling (RSC) is a commonly used ground-state cooling for trapped-ion qubits, but the cooling time scales up with numbers of ions due to its narrow cooling bandwidth. A further improvement of the conventional RSC is the parallel RSC, which shows a quadratic speedup for the cooling rate and a considerable extension for the cooling bandwidth [38]. However, it requires simultaneous single ion addressing technique, which is very challenging for large-size ion crystals.

*shuoshuo19851115@163.com
†pxchen@nudt.edu.cn
‡These authors contributed equally to this work.

EIT cooling is another widely used ground-state cooling technique. It employs a two-photon interference in a Λ configuration ion to tailor the absorption profile, which provides a faster method with a larger cooling bandwidth than RSC [39,40], such that motional modes within a certain range can be simultaneously cooled. The state-of-the-art experiment showed that the EIT cooling bandwidth can be extended up to more than 3 MHz by reducing the detunings of cooling beams [34]. However, the cooling bandwidth may still not be sufficient for cooling a large-size ion crystals. To seek a wider cooling bandwidth, one can use more energy levels than the simple Λ structure [e.g., double-EIT (Ref. [31,33])], but this scheme is atomic structure dependent and may still not be able to cover all the mode spectrum.

In this work, we theoretically propose and experimentally demonstrate a new EIT-like cooling method with arbitrary cooling bandwidth for trapped ions, which we refer to as the parallel EIT cooling method. The level structure involved in our scheme is similar to the standard EIT cooling. However, different from EIT cooling, the cooling resonance can be adjusted by both the ac Stark shift and the detuning difference between the driving beam and probe beam. This allows us to apply a range of probe laser beams with different detunings for multimode cooling. In this way, all the motional modes can be simultaneously cooled to the ground state, regardless of their mode separations. Compared with double EIT cooling [31,33], our scheme provides a broader cooling bandwidth and does not require additional energy levels. We experimentally demonstrate the scheme by cooling all motional modes of 1, 2, and 4 trapped $^{40}Ca^{+}$ ions to near ground state. We prove that our method has a cooling range more than 5 MHz by tuning the ac Stark shift and the mode frequency of a single ion. Moreover, our method shows no selectivity to the ion species since it requires only modulations of the probe beam compared to the EIT cooling.

II. THEORY AND SIMULATIONS

We first consider parallel EIT cooling of a single motional mode. The relevant levels involved in the parallel EIT scheme is the same as those in EIT cooling, as shown in Fig. 1(a). An ion with Λ configuration is confined in an ion trap with oscillation frequency ω. The probe laser and driving laser couple to transitions $|g\rangle \longleftrightarrow |e\rangle$ and $|r\rangle \longleftrightarrow |e\rangle$ with blue detunings Δ_g and Δ_r, Rabi frequencies Ω_g and Ω_r, respectively. In the rotation frame at the probe laser frequency, the Hamiltonian for atomic degrees of freedom (DOF) and motional DOF is

$$H_1 = -\Delta_g |e\rangle\langle e| - \Delta_{gr} |r\rangle\langle r| + \omega b^{\dagger} b, + \left(\frac{\Omega_g}{2} |e\rangle\langle g| + \frac{\Omega_r}{2} |e\rangle\langle r|\right) + \text{h.c.},$$

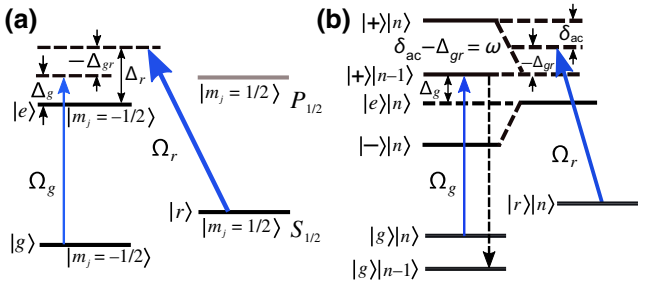

FIG. 1. (a) The relevant energy levels of the $^{40}Ca^{+}$ ion for implementing the parallel EIT cooling and EIT cooling. The ion has a dissipative excited state $|e\rangle$ and two ground states $|g\rangle$ and $|r\rangle$, transitions $|e\rangle \leftrightarrow |g\rangle$ and $|e\rangle \leftrightarrow |r\rangle$ are driven by a probe laser and a driving laser, respectively. When $\Delta_{gr} = 0$, the setup is for standard EIT cooling. (b) The cooling mechanism of parallel EIT cooling. Under the optimal cooling condition that $\Delta_{gr} - \delta_{ac} = -\omega$, the red sideband transition $|g, n\rangle \leftrightarrow |+, n-1\rangle$ is resonant.

where $\Delta_{gr} = \Delta_g - \Delta_r$ is the detuning difference, $b(b^{\dagger})$ is the annihilation (creation) operator of the ion's vibrational state. When $\Omega_g \ll \Omega_r$, a narrow-line dressed state $|+\rangle \approx \Omega_r |r\rangle + 2\delta_{ac} |e\rangle / \sqrt{\Omega_r^2 + 4\delta_{ac}^2}$ is generated by the strong coupling between $|r\rangle$ and $|e\rangle$, with $\delta_{ac} = \frac{1}{2}\left(\sqrt{\Omega_r^2 + \Delta_r^2} - |\Delta_r|\right) \approx \Omega_r^2 / (4|\Delta_r|)$ being the ac Stark shift created by driving laser, as shown in Fig. 1(b). The effective coupling $|g\rangle \longleftrightarrow |+\rangle$ creates a Fano-like absorption profile around Δ_r, where the absorption null and the narrow peak are at Δ_r and $\Delta_r + \delta_{ac}$, respectively.

In the Lamb-Dicke (LD) regime, the sideband interaction Hamiltonian is

$$H_{sb} = i\eta_{L1}\frac{\Omega_g}{2} |e\rangle\langle g| \left(b^{\dagger} + b\right) + \text{h.c.} + i\eta_{L2}\frac{\Omega_r}{2} |e\rangle\langle r| \left(b^{\dagger} + b\right) + \text{h.c.},$$

where η_{L1} and η_{L2} are Lamb-Dicke parameters of the two lasers along the motional axis. For $|\Delta_r| \gg \omega, |\Delta_{gr}|, \delta_{ac}$, one can neglect the transition from $|g\rangle$ to the far-detuned dressed state $|-\rangle$, and obtain the effective Hamiltonian

$$H_{sb,eff} = i\eta\frac{\Omega_+}{2} |+\rangle\langle g| \left(b^{\dagger} + b\right) + \text{h.c.}, \quad (1)$$

where $\eta = |\eta_{L1} - \eta_{L2}|$, $\Omega_+ = 2\Omega_g\delta_{ac}/\Omega_r$. Equation (1) contains the effective red sideband $|g\rangle|n\rangle \longrightarrow |+\rangle|n-1\rangle$ and blue sideband $|g\rangle|n\rangle \longrightarrow |+\rangle|n+1\rangle$, respectively.

In standard EIT cooling, the lasers are tuned to $\Delta_g = \Delta_r$, which corresponds to the EIT resonance that the atomic excitation is completely eliminated. One further tunes $\delta_{ac} = \omega$ such that the red sideband absorption falls at the peak of the profile, while the off-resonant blue sideband heating is suppressed. As a result, the ion is cooled to the ground state. However, note that it is not quite

necessary to completely eliminate the off-resonant carrier excitation, for its transition amplitude is negligible compared to that of red sideband transition. If we drop the constraint of EIT condition that $\Delta_g = \Delta_r$, and only address the red sideband resonance $|g\rangle\,|n\rangle \longrightarrow |+\rangle\,|n-1\rangle$, a more generalized cooling condition,

$$\Delta_{gr} - \delta_{\rm ac} = -\omega, \tag{2}$$

is obtained, as shown in Fig. 1(b). A detailed analytical cooling dynamics can be described by rate equation [41].

$$\frac{d}{dt}p_n = -\left[nA_- + (n+1)\,A_+\right]p_n + (n+1)\,A_-p_{n+1} + nA_+p_{n-1},$$

where p_n is the population of nth Fock state, and A_+ and A_- are heating and cooling coefficients. For $A_- > A_+$, the solution of the rate equation is

$$\langle n\,(t)\rangle = n_{\rm st} + (n_0 - n_{\rm st})\,e^{-Wt}, \tag{3}$$

where $\langle n\,(t)\rangle$ is the mean phonon occupation at time t, n_0 is the initial phonon occupation, $W = A_- - A_+$ is the cooling rate, and $n_{\rm st} = A_+/W$ is the steady mean phonon occupation. In weak sideband coupling regime, we can obtain $A_\pm$ of parallel EIT cooling by calculating the scattering amplitudes. The result shows that, under the optimal condition Eq. (2), the optimal cooling rate is $W = \eta^2\Omega_g^2/\gamma$, which is the same as that of standard EIT cooling. Meanwhile, the final mean phonon occupation of parallel EIT $n_{\rm st} = Rn_{\rm EIT}$, where $R = \left[1 + 4\alpha\,(1 - \delta_{\rm ac}/\omega)^2\right]$ is the ratio of $n_{\rm st}$ to EIT cooling $n_{\rm EIT} = \gamma^2/16\Delta_g^2$ under the same detuning Δ_g.

Compared with EIT cooling, the optimal condition Eq. (2) of parallel EIT cooling scheme provides a more flexible cooling resonance. In Figs. 2(a) and 2(b), we numerically compare the steady phonon occupations and cooling rates of parallel EIT cooling and standard EIT cooling for fixed Fano-like profile. In EIT cooling, detuning Δ_g has to be tuned equal to Δ_r, hence only the motional mode frequencies around $\delta_{\rm ac}$ are efficiently cooled. On the other hand, in parallel EIT cooling, by tuning Δ_{gr} to satisfy optimal cooling condition Eq. (2), the position of carrier transition can be adjusted, hence one can optimally cool the motional mode at arbitrary frequency. The results also show that parallel EIT cooling has a robust cooling over a large range of mode frequencies, which is especially useful for multimode cooling. Since each mode of an ion string can be cooled independently from the others in LD regime [42], cooling of multiple motional modes can be realized by applying a series of probe beams and one driving beam to cover the whole mode spectrum. The frequency of each probe beam is tuned to meet the optimal condition Eq. (2) to address one single mode or a range of nearby modes. In this way, all the modes are optimally cooled. Figure 2(c) shows an example of cooling the axial collective motions of a three-ion chain using parallel EIT cooling. One tunes the frequencies of three-probe beams such that the red sideband absorption of each mode is around the peak of the profile. To further highlight the cooling bandwidth, we align the positions of carrier absorptions, as shown in Fig. 2(d). There are three maxima, corresponding to red sideband resonance of the 3 modes.

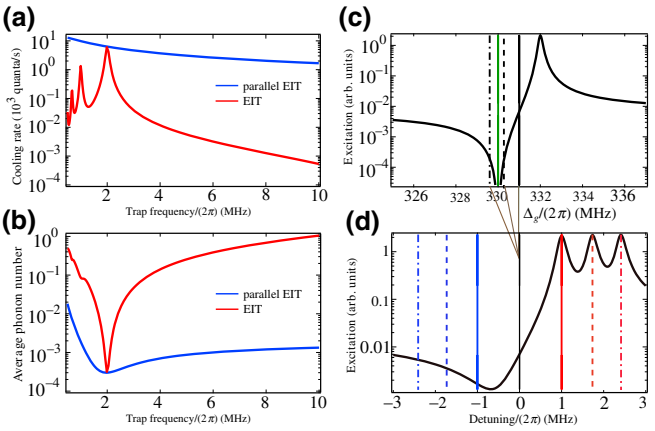

FIG. 2. (a),(b) Simulated final mean phonon numbers and cooling rate for cooling a single mode ω with parallel EIT cooling and EIT cooling (see Appendix A for more details). The varied mode frequency simulates the mode spectrum for multiple ions. The simulation parameters are $\Delta_r/(2\pi) = 330$ MHz, $\Omega_g/(2\pi) = 3$ MHz, and the effective LD parameter $\eta = 0.29/\sqrt{\omega/(2\pi)}$. The ac Stark shift is fixed at $\delta_{\rm ac}/(2\pi) = 2$ MHz. The probe beam has a constant detuning $\Delta_g = \Delta_r$ for the EIT cooling, while it is adjusted according to the condition Eq. (2) for parallel EIT cooling. (c) The Fano-like profile around EIT resonance. To simultaneous cool three separated modes at $\omega_1/(2\pi) = 1.0$ MHz, $\omega_2/(2\pi) = \sqrt{3}$ MHz, and $\omega_3/(2\pi) = \sqrt{29/5}$ MHz, one can apply three probe beams. Each beam is tuned to address one individual mode. The black vertical lines mark the probe laser detunings for the parallel EIT cooling and the green vertical line indicates the detuning for the EIT cooling. We further align the absorption spectra of the three beams at the carrier transition in (d). The three blue (red) vertical lines mark the positions of the blue (red) sidebands.

III. EXPERIMENTAL SETUP

We experimentally investigate parallel EIT cooling method on the dipole transition $S_{1/2} \leftrightarrow P_{1/2}$ of the $^{40}Ca^+$ ions at the wavelength of 397 nm and a natural linewidth of $\Gamma = 2\pi \times 20.7$ MHz. The whole setup is shown in Fig. 3(a). The ions are confined in a blade-shaped Paul trap with trap frequencies $2\pi \times (0.6 - 1.35)$ MHz along the axial direction and $2\pi \times (1.8 - 4.02)$ MHz for the transverse direction depending on the experiments. The relevant energy levels are formed by introducing a constant magnetic field $B_0 = 5.49$ G, which is at 45° with respect to the trap axis and results in a Zeeman shift of $\pm\Delta_B/2\pi =$

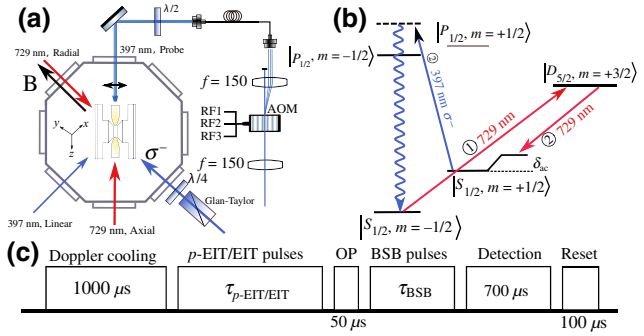

FIG. 3. (a) Geometric laser configurations for parallel-EIT cooling experiments. The parallel-EIT cooling requires both the σ^- beam and the probe beam, which is generated by injecting multiple rf frequencies to the single pass acoustic optical modulator (AOM). 397 linear beam is used for the Doppler cooling and fluorescence detection. The two 729 nm laser beams are used for the thermometry. (b) The scheme for the measurement of the ac Stark shift. The axial 729 laser beam stimulates the ion from $|S_{1/2}, m_j = -1/2\rangle$ to $|D_{5/2}, m_j = +3/2\rangle$ in the first step, then the driving beam are switched on while scanning the second 729 nm laser beam in second step, the ac Stark shift can be obtained by comparing the 729 nm laser frequency with and without the driving beam. (c) Experimental sequence to implement the EIT cooling and parallel-EIT cooling with trapped ions.

15.36 MHz between the states $|g\rangle$ and $|r\rangle$. The Λ system for one cooling resonance can be formed by using one of the probe beams and the driving beam, which are tuned near the two-photon resonance as depicted in Fig. 1(a). We couple the transition $|r\rangle \longleftrightarrow |e\rangle$ by a strong σ^- light with blue detuning up to $2\pi \times 330$ MHz. The weak π-polarized light couples the $|g\rangle \longleftrightarrow |e\rangle$ with a detuning difference Δ_{gr} to the σ^- light. In this case, the cooling bandwidth of a single EIT-like cooling is much narrower than the widely used setup [30,31,34], but the full motional spectrum can still be covered by using more probe beams, which proves the scalability of our scheme. Note that the wave-vector difference $\Delta\vec{k}$ between the driving and probe beams has components along all motional directions, therefore our setup can be used for cooling of all motional modes at the same time.

The ac Stark shift of the driving beam is determined by the spectroscopy of the quadrupole transition $S_{1/2} \leftrightarrow D_{5/2}$ as shown in Fig. 3(b). As the fact that the driving beam induces the same amount of ac Stark shift for states $|r\rangle$ and $|e\rangle$, the quadrupole transition frequency difference with and without driving beam is the ac Stark shift. Experimentally the measurement of σ^- beam induced ac Stark shift starts with preparing the ion in the state $|S_{1/2}, m_j = -1/2\rangle$, next the 729-nm π pulse flips the state to $|D_{5/2}, m_j = +3/2\rangle$, finally the driving beam and the 729-nm laser beam addressing the $|D_{5/2}, m_j = +3/2\rangle \leftrightarrow |S_{1/2}, m_j = 1/2\rangle$ are switched on simultaneously. The following measurement on the D state population is recorded as a function of the 729-nm laser frequency, the position with maximum absorption is the resonant frequency of the transition and the frequency shift from the case without pumping beam is the ac Stark shift.

The experimental sequence for testing the cooling method is shown in Fig. 3(c), we firstly use Doppler cooling to bring down the average phonon number of the ion to be around 10, then we switch on the cooling beams simultaneously for a fixed duration $\tau_{\text{parallel-EIT/EIT}}$, which is minimum time when EIT cooling on the target motional mode reaches cooling limit. Finally we apply a 50 μs optical pumping pulse to prepare the ion in the state $S_{1/2}(m_j = -1/2)$ and apply blue sideband pulses to measure the sideband spectroscopy of quadrupole transition $S_{1/2} \leftrightarrow D_{5/2}$ at 729 nm for thermometry. The final average phonon number $\bar{n}$ can be obtained by fitting experimental data points with the analytical solution of sideband Rabi oscillation [13,43].

IV. RESULTS

We perform proof of principle experiment on a single ion to study the optimal condition of the parallel-EIT cooling method and make a comparison for the cooling limit and bandwidth of the parallel-EIT cooling and EIT cooling. In Fig. 4(a), we measure the average phonon number of parallel-EIT cooling for different ac Stark shift δ_{ac}. The axial mode to be cooled has frequency $2\pi \times 1.35$ MHz and the optimal ac Stark shift for standard EIT cooling is $2\pi \times 1.35$ MHz. For parallel-EIT cooling method δ_{ac} is adjusted by tuning the Ω_r and the detuning Δ_g is chosen according to the optimal condition Eq. (2). For δ_{ac} ranging from 0.23 MHz to 5.25 MHz, we compare the cooling result with EIT cooling. The parallel-EIT cooling method shows a slight dependence on the ac Stark shift with best final phonon number around 0.05, while EIT cooling shows a limited cooling range as expected. We further investigate the cooling bandwidth of our method and EIT cooling by using fixed ac Stark shift and widely tuned mode frequencies, which simulate the mode spectrum of a string of ions. Figure 4(b) shows the cooling results of multiple modes with ac Stark shift fixed at $2\pi \times 1.2$ MHz, it can be seen that the final phonon number under different modes is almost the same for parallel EIT cooling, which agrees with theoretical prediction in Fig. 2(b).

We then investigate simultaneous cooling performance of parallel EIT cooling method by cooling all the modes of a single and two ions. For 3D cooling of a single ion, the σ^- light, which induces an ac Stark shift about $2\pi \times 2.0$ MHz, together with the π-polarized beam with two frequency components creates optimal cooling for trap frequencies $\{\omega_z, \omega_x, \omega_y\}/2\pi = \{0.6, 3.63, 3.71\}$ MHz. Figure 5(a) shows the cooling results for the three motional modes by applying a cooling pulse time of 1.5 ms. The average phonon numbers for all the motional modes are below 0.5. We also apply this method for cooling a

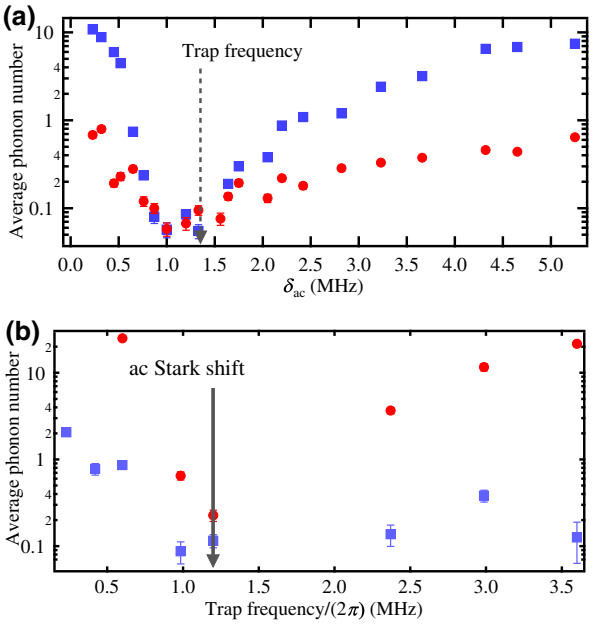

FIG. 4. (a) Cooling axial motional mode with frequency fixed at $\omega_z/2\pi = 1.35$ MHz. The blue square and red dots show the cooling results for the EIT cooling and parallel EIT cooling, respectively. (b) The cooling results for a fixed ac Stark shift at $\delta_{ac}/2\pi = 1.2$ MHz with variable motional frequencies. The parallel EIT cooling method shows almost the same cooling limit for a wide trap frequency range with the best average phonon number about 0.1, however the EIT cooling limit goes higher as the the trap frequency deviates from the fixed ac Stark shift.

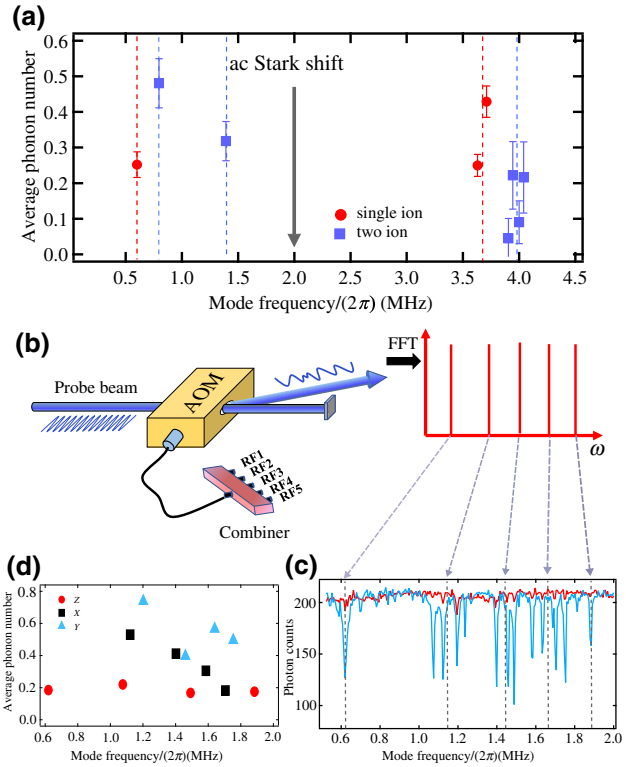

FIG. 5. (a) Mean phonon numbers for all motional modes of one and two $^{40}Ca^{+}$ ions after applying a cooling pulse of 1.5 *m*s. The vertical arrow shows the ac Stark shift at around $2\pi \times 2$ MHz. The red dots and blue squares show the average phonon numbers for the one- and two-ion cases, respectively. The vertical dash lines mark the cooling resonances. (b) The generation of probe beam for cooling a four-ion chain. Five rf signals with different frequencies are combined and then injected into a single-pass AOM to create a probe beam with five frequency components. (c) Blue and red sideband spectrum after applying the cooling pulses for a four-ion chain. The horizontal axis indicates the absolute detuning between the 729-nm laser and the carrier transition $S_{1/2}(m_j = -1/2) \leftrightarrow D_{5/2}(m_j = -3/2)$. The strong suppression of the red sideband transition indicates near ground-state cooling for all the motional modes. The dash lines denote the position of the cooling resonant frequencies. (d) The average phonon numbers for the 12 motional modes of the four-ion chain, thermometry for each motional mode is estimated using the sideband asymmetry and corresponding correction factor (see Appendix C for more details).

two-ion chain with trap frequencies $\{\omega_z, \omega_x, \omega_y\}/2\pi = \{0.8, 3.98, 4.02\}$ MHz, where three frequency components are added to the probe beam. The cooling results for two ions are also shown in Fig. 5(a), all the six motional modes are cooled down to near ground state with cooling time of 1.5 *m*s as the single-ion case. Note that the trap frequency difference for 1 and 2 ions is over 3 MHz, which is far beyond the cooling bandwidth of EIT cooling as indicated in Fig. 4(b), nevertheless, parallel EIT cooling method can cover all the motional modes.

We finally study the multimode cooling performance of our method by using a four-ion chain. To maintain the ion crystals in the trap, the trap frequencies are reduced to $\{\omega_z, \omega_x, \omega_y\}/2\pi = \{0.6, 1.706, 1.754\}$ MHz. To cover the whole mode spectrum, five frequency components are used for generating the probe beam (in practice, the number of the frequency components in probe beam can be reduced by lowering the detuning of the σ^- light) as shown in Fig. 5(b). With a cooling time of 1.5 *m*s, we observe an efficient simultaneous near ground-state cooling for all motional modes as indicated in Fig. 5(c) and more accurate average phonon numbers are shown in Fig. 5(d). The performance of parallel EIT cooling method is found to be the same for various ion numbers under the assumption that the probe beam has enough power for each frequency components. However, the reason why the final phonon number for multiple ions is not as low as the single-ion case has not be confirmed so far, which may be due to the heating and imperfect polarization of the beams, and will be left for our future work.

V. CONCLUSION

In summary, we propose an alternative cooling method with arbitrarily tunable cooling bandwidth. Experimentally we prove that the alternative cooling method is efficient

for the simultaneous cooling of multiple ions by using up to 4 $^{40}Ca^{+}$ ions and the parallel EIT cooling works well for the trap frequency down to 0.24 MHz, where the ion is far outside the LD regime. These experimental results showed the feasibility for simultaneous cooling for a large number of atoms and ions. Since realization of our method requires only modification on the probe beam compared to the standard EIT cooling, our scheme works as long as EIT works and therefore it is applicable for all currently operational trapped ion quantum computers [8–10]. In future work, we will try to cool a large number of ion crystals to see whether this method can fully replace the RSC.

ACKNOWLEDGMENTS

We thank Kihwan Kim, Yiheng Lin, Chu Guo for their helpful discussion. We acknowledge the use of the Quantum Toolbox in PYTHON (QuTiP) [44]. This work is supported by National Basic Research Program of China (Grant No. 2016YFA0301903), the National Natural Science Foundation of China (Grants No. 12004430, No. 11904402, No. 12074433, No. 12174447, No. 12174448, and No. 61632021). Innovation Program for Quantum Science and Technology (Grant No. 2021ZD0301600).

APPENDIX A: THEORETICAL MODEL OF PARALLEL-EIT COOLING

We consider that an ion of mass M is confined in a harmonic trap with trap frequency ω. The level configuration of the trapped ion can be treated as a three-level atom (see Fig. 6), with a dissipative excited state $|e\rangle$ and two ground states $|g\rangle$ and $|r\rangle$, whose level frequencies are ω_e, ω_g, and ω_r, respectively. States $|e\rangle$ and $|g\rangle$ couple to a cooling laser with frequency ω_{L1} and Rabi frequency Ω_g, while states $|e\rangle$ and $|r\rangle$ couple to a driving laser with frequency ω_{L2} and Rabi frequency Ω_r.

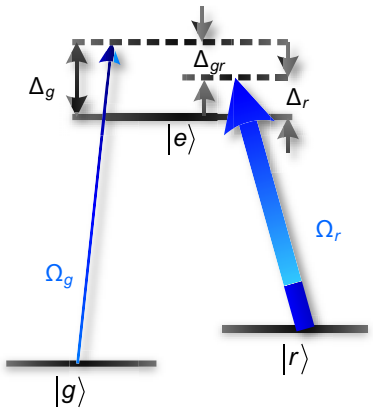

FIG. 6. The level diagram of the ion. The ion has a dissipative excited state $|e\rangle$ and two ground states $|g\rangle$ and $|r\rangle$, transitions $|e\rangle \leftrightarrow |g\rangle$ and $|e\rangle \leftrightarrow |r\rangle$ are driven by two external laser fields.

The Hamiltonian of the whole system takes the form

$$H = H_0 + V_{ge} + V_{re}, \tag{A1}$$

where H_0 is the free Hamiltonian of atomic DOF and motional DOF, V_{ge} (V_{re}) is the coupling between states $|g\rangle$ and $|e\rangle$ ($|e\rangle$ and $|r\rangle$), (we have set $\hbar = 1$)

$$\begin{aligned} H_0 &= -\Delta_g |e\rangle\langle e| - \Delta_{gr} |r\rangle\langle r| + \omega b^\dagger b, \\ V_{ge} &= \frac{\Omega_g}{2} |e\rangle\langle g| e^{ik_{L1}x\cos\varphi_g} + \text{h.c.}, \\ V_{re} &= \frac{\Omega_r}{2} |e\rangle\langle r| e^{ik_{L2}x\cos\varphi_r} + \text{h.c.} \end{aligned} \tag{A2}$$

Here $b(b^\dagger)$ is the annihilation (creation) operator of the ion's vibrational state; the detunings are defined by

$$\begin{aligned} \Delta_g &= \omega_{L1} - (\omega_e - \omega_g), \\ \Delta_r &= \omega_{L2} - (\omega_e - \omega_r), \\ \Delta_{gr} &= \Delta_g - \Delta_r; \end{aligned} \tag{A3}$$

the wave numbers are $k_{L1} = \frac{\omega_{L1}}{c}, k_{L2} = \frac{\omega_{L2}}{c}$; and φ_g (φ_r) denote the angle between the motional axis and cooling (driving) laser.

In the Lamb-Dicke (LD) regime, V_{ge} and V_{re} can be expanded to $V_{ge} = V_{ge}^0 + V_{ge}^1$ and $V_{re} = V_{re}^0 + V_{re}^1$, which are

$$\begin{aligned} V_{ge}^0 &= \frac{\Omega_g}{2} |e\rangle\langle g| + \text{h.c.}, \\ V_{re}^0 &= \frac{\Omega_r}{2} |e\rangle\langle r| + \text{h.c.}, \\ V_{ge}^1 &= i\eta_g \cos\varphi_g \frac{\Omega_g}{2} |e\rangle\langle g| \left(b^\dagger + b\right) + \text{h.c.}, \\ V_{re}^1 &= i\eta_r \cos\varphi_r \frac{\Omega_r}{2} |e\rangle\langle r| \left(b^\dagger + b\right) + \text{h.c.}, \end{aligned} \tag{A4}$$

where the superscript indicates the order in LD parameters, and

$$\eta_g = k_{L1}\sqrt{\frac{1}{2M\omega}}, \eta_r = k_{L2}\sqrt{\frac{1}{2M\omega}}. \tag{A5}$$

Then the Hamiltonian in LD regime reads

$$H_{\text{LD}} = H_0 + V_{ge}^0 + V_{re}^0 + V_{ge}^1 + V_{re}^1. \tag{A6}$$

By considering the dissipations, the master equation of the system is

$$\begin{aligned} \frac{d}{dt}\rho = -i[H,\rho] + \sum_{j=g,r} \frac{\gamma_j}{2} (2|j\rangle\langle e|\widetilde{\rho}|e\rangle\langle j| - |e\rangle\langle e|\rho \\ - \rho|e\rangle\langle e|), \end{aligned} \tag{A7}$$

where

$$|j\rangle\langle e|\widetilde{\rho}|e\rangle\langle j| = \frac{1}{2}\int_{-1}^{+1} d\left(\cos\theta_j\right)\mathcal{N}_j\left(\cos\theta_j\right) \times |j\rangle\langle e| e^{ik_{ej}x}\rho e^{-ik_{ej}x}|e\rangle\langle j|, \quad \text{(A8)}$$

with $\mathcal{N}_j\left(\cos\theta_j\right)$ being the angular distribution, and γ_j $(j = g, r)$ denotes the spontaneous dissipation rate from state $|e\rangle$ to $|j\rangle$.

Here, we are concerned with the regime where $\Omega_g \ll \Omega_r$, so that the atomic steady population is almost at state $|g\rangle$. In the LD regime, from the steady state of nth phonon $|g,n\rangle$, possible heating (cooling) transitions are

$$\begin{aligned}
&(a)\quad |g\rangle|n\rangle \xrightarrow{V_{ge}^0} |e\rangle|n\rangle \xrightarrow{\text{dissipation}} |g\rangle|n\pm1\rangle,\\
&(b)\quad |g\rangle|n\rangle \xrightarrow{V_{ge}^1} |e\rangle|n\pm1\rangle \xrightarrow{\text{dissipation}} |g\rangle|n\pm1\rangle,\\
&(c)\quad |g\rangle|n\rangle \xrightarrow{V_{ge}^0} |e\rangle|n\rangle \xrightarrow{V_{re}^0} |r\rangle|n\rangle \xrightarrow{V_{re}^1}\\
&\qquad |e\rangle|n\pm1\rangle \xrightarrow{\text{dissipation}} |g\rangle|n\pm1\rangle,\\
&(d)\quad |g\rangle|n\rangle \xrightarrow{V_{ge}^0} |e\rangle|n\rangle \xrightarrow{V_{re}^1} |r\rangle|n\pm1\rangle \xrightarrow{V_{re}^0}\\
&\qquad |e\rangle|n\pm1\rangle \xrightarrow{\text{dissipation}} |g\rangle|n\pm1\rangle, \quad \text{(A9)}
\end{aligned}$$

as depicted in Figs. 7(a)–7(d), respectively.

The cooling dynamics can be described by the rate equation for mean phonon number

$$\frac{d}{dt}\langle n\rangle = -\left(A_- - A_+\right)\langle n\rangle + A_+, \quad \text{(A10)}$$

where A_+ and A_- are the heating and cooling transition rates. For $A_- > A_+$, the solution of the rate equation is

$$\langle n(t)\rangle = n_{ss} + (n_0 - n_{ss})\, e^{-Wt}, \quad \text{(A11)}$$

where n_0 is the initial phonon number, $W = A_- - A_+$ is the cooling rate, and $n_{ss} = A_+/W$ is the steady mean phonon number.

In the weak sideband coupling regime, we can obtain $A_\pm$ by calculating all possible heating and cooling transitions [41,45,46] (A9), yielding

$$\begin{aligned}
A_- &= \alpha\gamma|\mathcal{T}_s|^2 + \gamma\left|\mathcal{T}_{1,-} + \mathcal{T}_{2,-} + \mathcal{T}_{3,-}\right|^2,\\
A_+ &= \alpha\gamma|\mathcal{T}_s|^2 + \gamma\left|\mathcal{T}_{1,+} + \mathcal{T}_{2,+} + \mathcal{T}_{3,+}\right|^2. \quad \text{(A12)}
\end{aligned}$$

The first term of A_- (A_+) denotes the cooling (heating) process caused by diffusion process [see Fig. 6(a)], and the second term corresponds to cooling (heating) process by three cooling (heating) sideband transitions [see Figs. 7(b)–7(d)]. Here,

$$\begin{aligned}
\mathcal{T}_s &= \frac{\eta_g\Omega_g}{2}\frac{\Delta_{gr}}{f(0)},\\
\mathcal{T}_{1,\pm} &= -i\eta_g\cos\varphi_g\frac{\Omega_g}{2}\frac{\mp\omega+\Delta_{gr}}{f(\mp\omega)},\\
\mathcal{T}_{2,\pm} &= -i\eta_r\cos\varphi_r\frac{\Omega_r\Omega_g}{4}\frac{\frac{\Omega_r}{2}}{f(0)}\frac{\mp\omega+\Delta_{gr}}{f(\mp\omega)},\\
\mathcal{T}_{3,\pm} &= i\eta_r\cos\varphi_r\frac{\Omega_r\Omega_g}{4}\frac{\Delta_{gr}}{f(0)}\frac{\frac{\Omega_r}{2}}{f(\mp\omega)}, \quad \text{(A13)}
\end{aligned}$$

with

$$f(x) = \left(\Delta_g + x\right)\left(\Delta_{gr} + x\right) - \frac{\Omega_r^2}{4} + i\frac{\left(\Delta_{gr}+x\right)\gamma}{2}, \quad \text{(A14)}$$

and $\alpha = \int_{-1}^{+1} d\left(\cos\theta_j\right)\cos^2\theta_j\mathcal{N}_j\left(\cos\theta_j\right)$.

Efficient cooling is achieved by enhancing cooling transition rate A_- while suppressing A_+. For a sufficiently strong coupling Ω_r, cooling transition rate A_- reaches its maximum value at

$$\mathrm{Re}f(\nu) = \left(\Delta_g + \omega\right)\left(\Delta_{gr} + \omega\right) - \frac{\Omega_r^2}{4} = 0, \quad \text{(A15)}$$

where the denominator of A_- is minimum. This can be understood in dressed-state representation. As $\Omega_g \ll \Omega_r$, dressed states $|+\rangle$ and $|-\rangle$ are created by driving beam, which are

$$\begin{aligned}
|+\rangle &= \sin\phi|e\rangle - \cos\phi|r\rangle,\\
|-\rangle &= \cos\phi|e\rangle + \sin\phi|r\rangle, \quad \text{(A16)}
\end{aligned}$$

with $\phi = \frac{1}{2}\arctan|\Omega_r|/\Delta_r$. The corresponding energies of $|+\rangle$ and $|-\rangle$ are

$$E_\pm = \frac{1}{2}\left(-\Delta_r \pm \sqrt{\Omega_r^2 + \Delta_r^2}\right). \quad \text{(A17)}$$

By tuning the cooling laser in resonance with red sideband transition of the narrow-line dressed state $|+\rangle$, i.e., $|g\rangle|n\rangle \longrightarrow |+\rangle|n-1\rangle$, detunings should satisfy

$$\left|\Delta_{gr} + \omega\right| = \delta_{\mathrm{ac}}. \quad \text{(A18)}$$

One can verify that the red sideband resonance condition is precisely the same as optimal condition (A15).

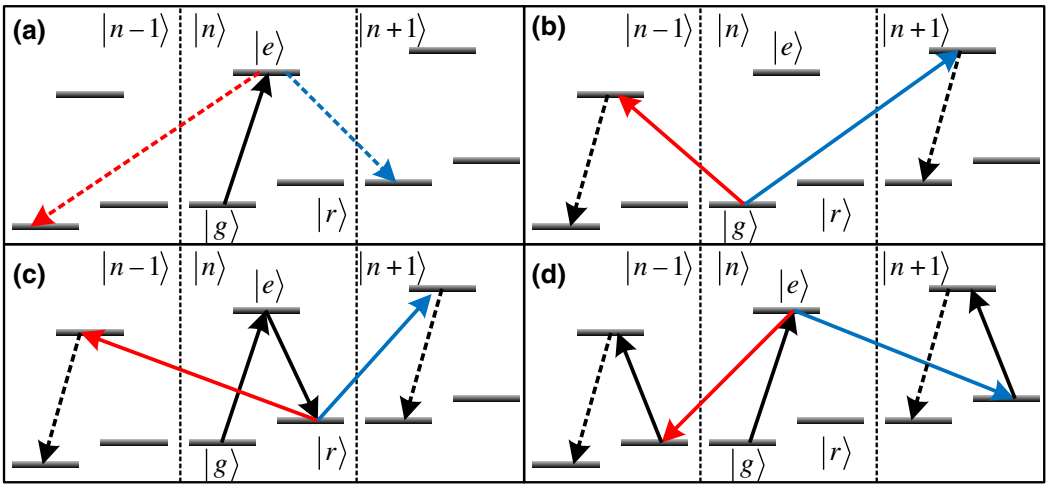

FIG. 7. The possible cooling and heating transitions. (a)–(d) correspond to transitions (a)–(d) in Eq. (A9).

Assuming that $|\Delta_g| \gg \omega, |\Delta_{gr}|, \delta_{\rm ac}$, we obtain

$$A_- \simeq \eta_1^2 \frac{\Omega_g^2}{\gamma},$$
$$A_+ \simeq \eta_2^2 \left(\frac{\gamma \Omega_g^2}{16\Delta_g^2}\right),$$

with the effective Lamb-Dicke parameters η_1 and η_2 defined by

$$\eta_1^2 = \eta^2,$$
$$\eta_2^2 = \begin{cases} \eta^2\left(1+4\alpha\left(1-\frac{\delta_{\rm ac}}{\omega}\right)^2\right) & \Delta_g > 0, \\ \eta^2\left(1+4\alpha\left(1+\frac{\delta_{\rm ac}}{\omega}\right)^2\right) & \Delta_g < 0. \end{cases}$$

Here, we define that $\eta_g \approx \eta_r = \eta/2$, and assume $\varphi_g = 0, \varphi_r = \pi$ for simplicity. The corresponding final mean phonon number is

$$n_{st} = R n_{\rm EIT},$$

where R is the ratio of parallel EIT cooling's $n_{\rm st}$ to EIT cooling $n_{\rm EIT} = \gamma^2/16\Delta_g^2$, that is

$$R = \begin{cases} 1+4\alpha\left(1-\frac{\delta_{\rm ac}}{\omega}\right)^2 & \Delta_g > 0, \\ 1+4\alpha\left(1+\frac{\delta_{\rm ac}}{\omega}\right)^2 & \Delta_g < 0. \end{cases}$$

APPENDIX B: MULTIMODE COOLING VIA PARALLEL EIT COOLING

To theoretical analysis of multimode cooling via parallel EIT cooling, we first consider the simplest case that cooling of a single ion's two-dimensional (2D) motion with two separated motional modes. We apply two-probe laser beams and one driving beam. The interaction Hamiltonian takes the form

$$H = H_0 + V.$$

Here, H_0 is the free Hamiltonian for atomic DOF and motional DOF

$$H_0 = \omega_z a_z^\dagger a_z + \omega_x a_x^\dagger a_x - \Delta_{g1} |e\rangle\langle e| - \Delta_{g1r} |r\rangle\langle r|,$$

where Δ_{g1} is the detuning of the first probe laser, $\Delta_{g1r} = \Delta_{g1} - \Delta_r$, and ω_z and ω_x are the trap frequencies of axial and radial modes.

The laser-ion interaction term V is

$$\begin{aligned} V = {} & \frac{\Omega_{g1}}{2} |e\rangle\langle g| \exp\left[i\sum_{k=x,z}\eta_{gk}\left(a_k + a_k^\dagger\right)\cos\theta_{k1}\right] \\ & + \frac{\Omega_{g2}}{2} |e\rangle\langle g| \exp \\ & \times \left[i\sum_{k=x,z}\eta_{gk}\left(a_k + a_k^\dagger\right)\cos\theta_{k2} + i\Delta_{g12}t\right] \\ & + \frac{\Omega_r}{2} |e\rangle\langle r| + \text{h.c.}, \end{aligned} \tag{B1}$$

where $\Delta_{g12} = \Delta_{g1} - \Delta_{g2}$ is the frequency difference between the detunings of two probe lasers, Δ_{g2} is the detuning of the second probe laser; $\eta_{gk} = k_L\sqrt{1/2M\omega_k}\,(k = x, z)$; θ_{kl} is the angle between the lth probe laser and k axis. For simplicity, we assume that the driving laser is perpendicular to the two axes. In dressed-state basis and the interaction picture, the Hamiltonian

takes the form

$$H = \frac{\Omega_{+1}}{2}|+\rangle\langle g|\exp \times\left[i\sum_{k=x,z}\eta_{gk}\left(a_k e^{-i\omega_k t}+a_k^{\dagger}e^{i\omega_k t}\right)\cos\theta_{k1}\right] \times e^{i(-\Delta_{g1r}+\delta_{\rm ac})t}+\text{h.c.} + \frac{\Omega_{+2}}{2}|+\rangle\langle g|\exp \times\left[i\sum_{k=x,z}\eta_{gk}\left(a_k e^{-i\omega_k t}+a_k^{\dagger}e^{i\omega_k t}\right)\cos\theta_{k2}\right] \times e^{i(-\Delta_{g2r}+\delta_{\rm ac})t}+\text{h.c.}, \quad \text{(B2)}$$

where we neglect the far-off resonant state $|-\rangle$.

In the LD regime, by tuning that

$$\Delta_{g1r}+\omega_z=\Delta_{g2r}+\omega_x=\delta_{\rm ac} \quad \text{(B3)}$$

and neglecting off-resonant transitions, we obtain the effective Hamiltonian

$$H_{\rm eff}=i\eta_{gz}\frac{\Omega_{+1}}{2}|+\rangle\langle g|a_z+\text{h.c.} + i\eta_{gx}\frac{\Omega_{+2}}{2}|+\rangle\langle g|a_x+\text{h.c.} \quad \text{(B4)}$$

In weak coupling regime, either mode is cooled independently from the other [Fig. 8(a)]. However, due to the multiphonon resonances, the whole system may evolve into some dark states, e.g., $\alpha_1|g,2_x,0_z\rangle+\alpha_2|g,1_x,1_z\rangle+\alpha_3|g,0_x,2_z\rangle$, which decouples from the $H_{\rm eff}$. To avoid the dark resonance, we can set the detunings such that conditions (B3) are slightly mismatched, i.e.,

$$\Delta_{g1r}+\omega_z+\varepsilon=\Delta_{g2r}+\omega_x-\varepsilon=\delta_{\rm ac},$$

where $|\varepsilon|\ll\omega_{x,z}$. This way, the 2D motion can be cooled at the same time.

In Fig. 8(b), we numerically simulate the simultaneous 2D cooling. To highlight the advantage of our scheme, we consider an extreme case that $\omega_x=10\omega_z$, where standard EIT cooling have to sequentially cool the two modes. We also plot parallel EIT cooling of single mode for comparison. The simulation shows that the simultaneous 2D cooling has the same cooling rates as those of single mode cooling.

We further consider that an N-ion chain with $3N$ collective modes are globally coupled by m probe lasers and one

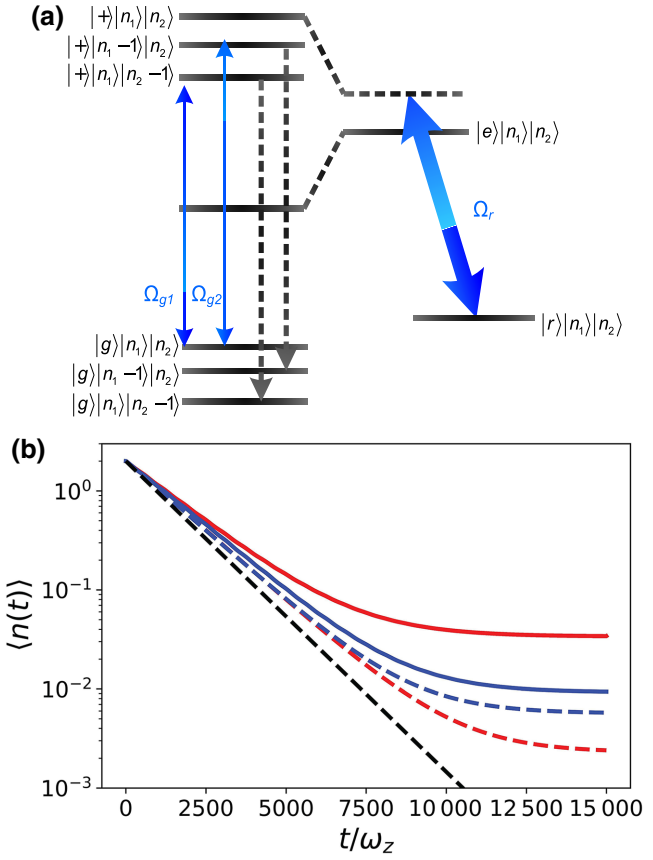

FIG. 8. (a) Cooling principle for simultaneously cooling 2D motional modes of a single ion. Two probe laser beams and one driving beam create cooling resonances for the widely separated axial mode (ω_z) and radial mode (ω_x). (b) The average photon number $\langle n(t)\rangle$ as a function of t for multimode parallel EIT cooling. The red and blue solid lines are simultaneously cooling dynamics for axial mode and radial mode, respectively. The red and blue dashed lines correspond to the cooling dynamics of single-mode cooling at the same parameters. The black dashed line is the analytical prediction. The simulation parameters are $\omega_x=10\omega_z$, $\delta_{\rm ac}=2\omega_z$, $\Delta_r=330\omega_z$, $\gamma=20\omega_z$, $\Omega_{g1}=\omega_z$,$\Delta_{g1}=(331+0.005)\,\omega_z$, $\Omega_{g2}=3.16\omega_z$, $\Delta_{g2}=(322-0.005)\,\omega_z$, $\eta_{gz}=0.17$, $\theta_{k1}=\theta_{k2}=\pi/4$.

driving laser. The Hamiltonian takes the form

$$H=\sum_{j=1}^{N}\sum_{l=1}^{m}\frac{\Omega_{+l}}{2}|+\rangle_{jj}\langle g|\exp\left[i\sum_{k=1}^{3N}\eta_{jk}\left(a_k e^{-i\omega_k t}+a_k^{\dagger}e^{i\omega_k t}\right)\right]e^{i(-\Delta_{glr}+\delta_{\rm ac})t}+\text{h.c.}, \quad \text{(B5)}$$

where the indices j,k,l indicate the jth ion, kth collective mode and lth probe laser, $\eta_{jk}=k_L\sqrt{1/2M\omega_k}b_{jk}$ with b_{jk} being the eigenvectors for the mode k. One can tune the frequencies of probe lasers, such that each probe laser is tuned to near resonance with the red sideband transition for a range of nearby modes. As a result, all the

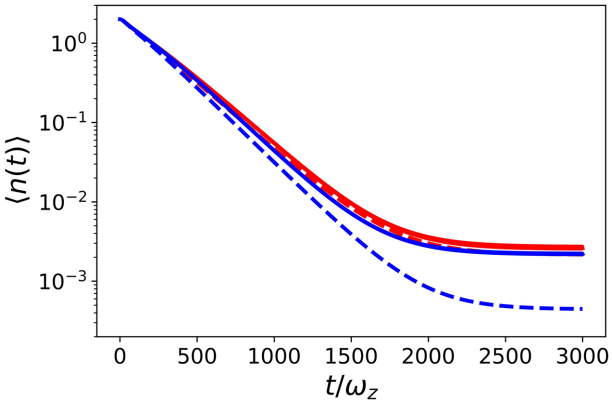

FIG. 9. The average photon number $\langle n\,(t)\rangle$ as a function of t for simultaneous cooling two axial modes of a two-ion crystal. The red and blue solid lines stand for center-of-mass mode (ω_z) and stretch mode ($\sqrt{3}\omega_z$). The dashed lines correspond to the cooling dynamics of single-mode cooling at the same parameters. The simulation parameters are $\delta_{\rm ac} = 2\omega$, $\Delta_r = 330\omega$, $\gamma = 20\omega_z$, $\Omega_{g1} = \omega_z$, $\Delta_{g1} = (331 + 0.005)\,\omega_z$, $\Omega_{g2} = 1.32\omega_z$, $\Delta_{g2} = (330.27 - 0.005)\,\omega_z$, $\eta_{\rm COM} = 0.24$, $\eta_{\rm strech} = 0.18$.

motional modes can be cooled near the ground state. However, each of the modes may be affected by heating effects from all probe lasers. The heating coefficient of the mode at frequency ω is $A_+\,(\omega) = \sum_{l=1}^{m} A_{+l}\,(\omega)$, where

$$A_{+l} \sim \gamma_+ \eta^2 \left(\frac{\Omega_{l+}}{2}\right)^2 \left[\frac{\alpha\left(\frac{\Delta_{glr}}{\omega}\right)^2}{\left(\Delta_{glr} - \delta_{\rm ac}\right)^2 + \frac{\gamma_+^2}{4}\left(\frac{\Delta_{glr}}{\omega}\right)^2} + \frac{\left(\frac{\Delta_{glr}-\omega}{\omega}\right)^2}{\left(\Delta_{glr} - \delta_{\rm ac} - \omega\right)^2 + \frac{\gamma_+^2}{4}\left(\frac{\Delta_{glr}-\omega}{\omega}\right)^2}\right].$$

Therefore, the final mean phonon number roughly scales linearly with the number of the probe beams.

In Fig. 9, we demonstrate the numerical simulation of the simultaneous cooling two axial modes of a two-ion crystal. The two ions are globally coupled by two probe lasers. For both of the probe lasers illuminate the two ions, the cooling rate of the ion string is the same as that of cooling a single ion.

For cooling all motional modes of a long ion string, we need to consider the size of the ion crystal since our method works in the LD regime. Assuming cooling of a linear string of 40 ion with transverse trap frequency about 4.5 MHz as in Ref. [34], the maximum axial center of mass (COM) mode frequency to keep the linear string is about 280 kHz according to the theory in Ref. [17], in this case the average phonon number would be quite high after Doppler cooling, our method cannot be applied since the ions are far from LD regime, therefore the cooling mode frequency of our method cannot be arbitrarily low. Experimentally the cooling bandwidth of our method can be further extended with the help of sub-Doppler cooling method such as Sisyphus cooling.

APPENDIX C: THERMOMETRY THEORY FOR MULTIPLE ION

For one and two ions, the average phonon number after cooling can be found by using the motional sensitive Rabi oscillation since the analytical solution of the blue sideband Rabi oscillation can be found [13] by the laser-atom interaction Hamiltonian. Alternatively the cooling results for a motional mode can also be measured by using the sideband spectroscopy, which includes the measurement on the blue and red sideband. Under the assumption of thermal distribution, the average phonon number $\bar{n}$ for a single ion can be extracted by using the sideband asymmetry $p_r/(p_b - p_r)$, where $\bar{n} = p_r/(p_b - p_r)$, p_b and p_r are the probability of blue- and red-sideband Rabi oscillations [43]. For an ion chain with more than two ions, there is only numerical solutions for the Rabi oscillation. Instead of fitting to the sideband Rabi oscillation, we use numerical simulations to find the correction factor for sideband thermometry method such that the average phonon number is estimated to be the product of the sideband asymmetry and the correction factor.

In our experiment, we choose $|S_{1/2}(m_j = -1/2)\rangle$ ($|\downarrow\rangle$) and $|D_{5/2}, m_j = -3/2\rangle$ ($|\uparrow\rangle$) as the qubit states. A 729-nm laser beam shining the ions globally with the same intensity is used to drive the quadrupole transition. The detuning δ is the frequency difference between the 729-nm laser and qubit transition.

In the Lamb-Dicke regime, which is always the case after the precooling, the laser-atom interaction Hamiltonian can be expressed as

$$H_I = \frac{\hbar\Omega}{2}\sum_{j=1}^{N}\sigma_{+j}\exp\Big[i\sum_{k=1}^{3N}\eta_{jk}(a_k e^{-i\omega_k t} + a_k^\dagger e^{i\omega_k t}) - i(\Delta t - \phi_j)\Big] + \text{h.c.}, \tag{C1}$$

where k and j indicate the collective mode and ion number, respectively. Ω is the Rabi frequency, $\eta_{jk} = 2\pi/\lambda\sqrt{\hbar/2m\omega_k}b_{jk}$ is the Lamb-Dicke parameter, where m is the mass of $^{40}Ca^+$ ion, ω_k is the mode frequency, λ is the wavelength of 729-nm laser, and b_{jk} is the eigenvectors for the mode k. σ is the operator for qubit and a ($a^\dagger$) is the annihilation (creation) operator.

When the detuning Δ is set at the frequency of a motional mode ω_k ($-\omega_k$), the Hamiltonian H_I can be simplified to

$$H_{r,k} = \frac{i\hbar\Omega}{2}\sum_{j=1}^{N}\sigma_{+j}\eta_{jk}a_k + \text{h.c.}, \tag{C2}$$

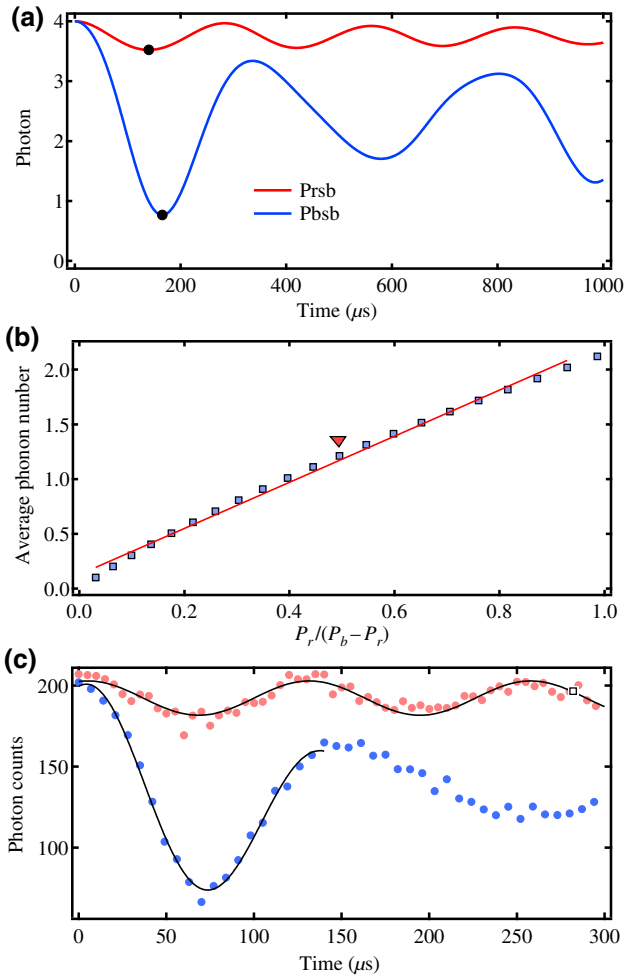

FIG. 10. (a) Simulation of Rabi oscillations for blue- (blue curve) and red-sideband (red curve) transitions of the radial COM mode with average phonon number of 0.5. The black dots show the π-pulse positions of the Rabi oscillations, which is used to calculate the sideband asymmetry $p_r/(p_b - p_r)$. (b) Simulated average phonon number as a function of the sideband asymmetry. The blue squares are the simulation results and the red line shows the linear fit for extracting the correction factor. (c) Experimental results for Rabi oscillation of the radial asymmetry mode. The transition amplitude for blue-and red-sideband cooling is found to be 129 and 21 from the fitting and the average phonon number is calculated to be 0.40 based on the correction factor found in Table I.

$$H_{b,k} = \frac{i\hbar\Omega}{2}\sum_{j=1}^{N}\sigma_{+j}\,\eta_{jk}a_k^{\dagger} + \text{h.c.}, \tag{C3}$$

where $H_{r,k}$ and $H_{b,k}$ are Hamiltonians for the red and blue sideband transitions.

By numerically solving the Schrödinger equations of red- and blue-sideband transitions under the initial state $|\downarrow\downarrow\cdots\downarrow, n_k\rangle$, where $|n_k\rangle$ is the Fock state of mode k, we can obtain the time evolution of the upstate of the ions $P_{\uparrow,n_k}(t)$ [17,31]. Assuming the thermal state distribution for the phonons, we can find the time evolution of $P_{\uparrow,n_k}(t)$ as a function of the average phonon number $\bar{n}_k$. Similar to the single-ion case, we can use the sideband spectroscopy and a mode-dependent factor to get the approximate evaluation of average phonon number $\bar{n}_k$. The factor can be extracted by fitting the numerical found $p_r/(p_b - p_r)$ versus $\bar{n}_k$. Considering four ions with trap frequencies $\{\omega_z, \omega_x, \omega_y\}/2\pi = \{0.6, 1.706, 1.754\}$ MHz, the mode-dependent factor is found as shown in Table I, Fig. 10(a) is the simulated Rabi oscillation for the red- and blue-sideband transition of radial COM mode with average phonon number of 0.5. Figure 10(b) shows the linear fit for extracting the correction factor of the radial COM mode, and the correction factor is found to be 2.10. As an example we extract the phonon number of the radial asymmetry mode by fitting the blue- and red-sideband Rabi oscillation as shown in Fig. 10(c). Based on the amplitude of the fitting function and correction factor above, the final phonon number is calculated to be 0.4.

TABLE I. Simulated mode-dependent correction factor for a four-ion chain.

Motional mode	X	Y	Z
COM	2.10(4)	2.10(4)	2.11(4)
Symmetric stretch	2.471(6)	2.471(6)	2.363(9)
Asymmetric stretch	2.06(3)	2.06(3)	2.04(3)
Zigzag	2.484(6)	2.484(6)	2.463(6)

[1] D. Porrasand and J. I. Cirac, Effective Quantum Spin Systems with Trapped Ions, Phys. Rev. Lett. **92**, 207901 (2004).
[2] R. Blattand and C. F. Roos, Quantum simulations with trapped ions, Nat. Phys. **8**, 277 (2012).
[3] A. Ruiz, D. Alonso, M. B. Plenio, and A. del Campo, Tuning heat transport in trapped-ion chains across a structural phase transition, Phys. Rev. B **89**, 214305 (2014).
[4] D. J. Wineland, Nobel lecture: Superposition, entanglement, and raising Schrödinger's cat, Rev. Mod. Phys. **85**, 1103 (2013).
[5] Y. Pan, J. Zhang, E. Cohen, C.-w. Wu, P.-X. Chen, and D. Nir, Weak-to-strong transition of quantum measurement in a trapped-ion system, Nat. Phys. **16**, 1206 (2020).
[6] J. I. Ciracand and P. Zoller, Quantum Computations with Cold Trapped Ions, Phys. Rev. Lett. **74**, 4091 (1995).
[7] C.-W. Wu, J. Zhang, Y. Xie, B.-Q. Ou, T. Chen, W. Wu, and P.-X. Chen, Scheme and experimental demonstration of fully atomic weak-value amplification, Phys. Rev. A **100**, 062111 (2019).
[8] J. M. Pino, J. M. Dreiling, C. Figgatt, J. P. Gaebler, S. A. Moses, M. Allman, C. Baldwin, M. Foss-Feig, D.

Hayes, and K. Mayer, *et al.*, Demonstration of the trapped-ion quantum CCD computer architecture, Nature **592**, 209 (2021).

[9] L. Egan, D. M. Debroy, C. Noel, A. Risinger, D. Zhu, D. Biswas, M. Newman, M. Li, K. R. Brown, and M. Cetina, *et al.*, Fault-tolerant control of an error-corrected qubit, Nature **598**, 281 (2021).

[10] I. Pogorelov, T. Feldker, C. D. Marciniak, L. Postler, G. Jacob, O. Krieglsteiner, V. Podlesnic, M. Meth, V. Negnevitsky, M. Stadler, B. Höfer, C. Wächter, K. Lakhmanskiy, R. Blatt, P. Schindler, and T. Monz, Compact Ion-Trap Quantum Computing Demonstrator, PRX Quantum **2**, 020343 (2021).

[11] C. J. Ballance, T. P. Harty, N. M. Linke, M. A. Sepiol, and D. M. Lucas, High-Fidelity Quantum Logic Gates using Trapped-Ion Hyperfine Qubits, Phys. Rev. Lett. **117**, 060504 (2016).

[12] T. P. Harty, M. A. Sepiol, D. T. C. Allcock, C. J. Ballance, J. E. Tarlton, and D. M. Lucas, High-Fidelity Trapped-Ion Quantum Logic using Near-Field Microwaves, Phys. Rev. Lett. **117**, 140501 (2016).

[13] B. E. King, C. S. Wood, C. J. Myatt, Q. A. Turchette, D. Leibfried, W. M. Itano, C. Monroe, and D. J. Wineland, Cooling the Collective Motion of Trapped Ions to Initialize a Quantum Register, Phys. Rev. Lett. **81**, 1525 (1998).

[14] T. P. Harty, D. T. C. Allcock, C. J. Ballance, L. Guidoni, H. A. Janacek, N. M. Linke, D. N. Stacey, and D. M. Lucas, High-Fidelity Preparation, Gates, Memory, and Readout of a Trapped-Ion Quantum Bit, Phys. Rev. Lett. **113**, 220501 (2014).

[15] M. Brownnutt, M. Kumph, P. Rabl, and R. Blatt, Ion-trap measurements of electric-field noise near surfaces, Rev. Mod. Phys. **87**, 1419 (2015).

[16] Q. A. Turchette, C. J. Myatt, B. E. King, C. A. Sackett, D. Kielpinski, W. M. Itano, C. Monroe, and D. J. Wineland, Decoherence and decay of motional quantum states of a trapped atom coupled to engineered reservoirs, Phys. Rev. A **62**, 053807 (2000).

[17] S. Ejtemaee, *Dynamics of Trapped Ions Near the Linear-Zigzag Structural Phase Transition*, Ph.d thesis, Simon Fraser University (2015).

[18] M. Cetina, L. Egan, C. Noel, M. Goldman, A. Risinger, D. Zhu, D. Biswas, and C. Monroe, Quantum gates on individually-addressed atomic qubits subject to noisy transverse motion, (2020), arXiv preprint ArXiv:2007.06768.

[19] D. J. Winelandand and W. M. Itano, Laser cooling of atoms, Phys. Rev. A **20**, 1521 (1979).

[20] S. Stenholm, The semiclassical theory of laser cooling, Rev. Mod. Phys. **58**, 699 (1986).

[21] J. Dalibardand and C. Cohen-Tannoudji, Laser cooling below the doppler limit by polarization gradients: Simple theoretical models, J. Opt. Soc. Am. B **6**, 2023 (1989).

[22] Z.-C. Mao, Y.-Z. Xu, Q.-X. Mei, W.-D. Zhao, Y. Jiang, Y. Wang, X.-Y. Chang, L. He, L. Yao, Z.-C. Zhou, Y.-K. Wu, and L.-M. Duan, Experimental Realization of Multi-Ion Sympathetic Cooling on a Trapped Ion Crystal, Phys. Rev. Lett. **127**, 143201 (2021).

[23] M. Joshi, A. Fabre, C. Maier, T. Brydges, D. Kiesenhofer, H. Hainzer, R. Blatt, and C. Roos, Polarization-gradient cooling of 1D and 2D ion Coulomb crystals, New J. Phys. **22**, 103013 (2020).

[24] S. Ejtemaeeand and P. C. Haljan, 3D Sisyphus Cooling of Trapped Ions, Phys. Rev. Lett. **119**, 043001 (2017).

[25] F. Diedrich, J. C. Bergquist, W. M. Itano, and D. J. Wineland, Laser Cooling to the Zero-Point Energy of Motion, Phys. Rev. Lett. **62**, 403 (1989).

[26] C. Roos, T. Zeiger, H. Rohde, H. C. Nägerl, J. Eschner, D. Leibfried, F. Schmidt-Kaler, and R. Blatt, Quantum State Engineering on an Optical Transition and Decoherence in a Paul Trap, Phys. Rev. Lett. **83**, 4713 (1999).

[27] C. Monroe, D. M. Meekhof, B. E. King, S. R. Jefferts, W. M. Itano, D. J. Wineland, and P. Gould, Resolved-Sideband Raman Cooling of a Bound Atom to the 3D Zero-Point Energy, Phys. Rev. Lett. **75**, 4011 (1995).

[28] G. Morigi, J. Eschner, and C. H. Keitel, Ground State Laser Cooling using Electromagnetically Induced Transparency, Phys. Rev. Lett. **85**, 4458 (2000).

[29] C. F. Roos, D. Leibfried, A. Mundt, F. Schmidt-Kaler, J. Eschner, and R. Blatt, Experimental Demonstration of Ground State Laser Cooling with Electromagnetically Induced Transparency, Phys. Rev. Lett. **85**, 5547 (2000).

[30] R. Lechner, C. Maier, C. Hempel, P. Jurcevic, B. P. Lanyon, T. Monz, M. Brownnutt, R. Blatt, and C. F. Roos, Electromagnetically-induced-transparency ground-state cooling of long ion strings, Phys. Rev. A **93**, 053401 (2016).

[31] M. Qiao, Y. Wang, Z. Cai, B. Du, P. Wang, C. Luan, W. Chen, H.-R. Noh, and K. Kim, Double-Electromagnetically-Induced-Transparency Ground-State Cooling of Stationary Two-Dimensional Ion Crystals, Phys. Rev. Lett. **126**, 023604 (2021).

[32] E. Jordan, K. A. Gilmore, A. Shankar, A. Safavi-Naini, J. G. Bohnet, M. J. Holland, and J. J. Bollinger, Near Ground-State Cooling of Two-Dimensional Trapped-Ion Crystals with More than 100 Ions, Phys. Rev. Lett. **122**, 053603 (2019).

[33] N. Scharnhorst, J. Cerrillo, J. Kramer, I. D. Leroux, J. B. Wübbena, A. Retzker, and P. O. Schmidt, Experimental and theoretical investigation of a multimode cooling scheme using multiple electromagnetically-induced-transparency resonances, Phys. Rev. A **98**, 023424 (2018).

[34] L. Feng, W. L. Tan, A. De, A. Menon, A. Chu, G. Pagano, and C. Monroe, Efficient Ground-State Cooling of Large Trapped-Ion Chains with an Electromagnetically-Induced-Transparency Tripod Scheme, Phys. Rev. Lett. **125**, 053001 (2020).

[35] Y. Lin, J. P. Gaebler, T. R. Tan, R. Bowler, J. D. Jost, D. Leibfried, and D. J. Wineland, Sympathetic Electromagnetically-Induced-Transparency Laser Cooling of Motional Modes in an Ion Chain, Phys. Rev. Lett. **110**, 153002 (2013).

[36] S. Webster, *Raman Sideband Cooling and Coherent manipulation of trapped ions*, PhD thesis, University of Oxford (2005).

[37] T. Kampschulte, W. Alt, S. Manz, M. Martinez-Dorantes, R. Reimann, S. Yoon, D. Meschede, M. Bienert, and G. Morigi, Electromagnetically-induced-transparency control

of single-atom motion in an optical cavity, Phys. Rev. A **89**, 033404 (2014).

[38] J.-S. Chen, K. Wright, N. C. Pisenti, D. Murphy, K. M. Beck, K. Landsman, J. M. Amini, and Y. Nam, Efficient-sideband-cooling protocol for long trapped-ion chains, Phys. Rev. A **102**, 043110 (2020).

[39] S. Zhang, J.-Q. Zhang, W. Wu, W.-S. Bao, and C. Guo, Fast cooling of trapped ion in strong sideband coupling regime, New J. Phys. **23**, 023018 (2021).

[40] X.-Q. Li, S. Zhang, J. Zhang, W. Wu, C. Guo, and P.-X. Chen, Fast laser cooling using optimal quantum control, Phys. Rev. A **104**, 043106 (2021).

[41] J. I. Cirac, R. Blatt, P. Zoller, and W. D. Phillips, Laser cooling of trapped ions in a standing wave, Phys. Rev. A **46**, 2668 (1992).

[42] G. Morigiand and J. Eschner, Is an ion string laser-cooled like a single ion?, J. Phys. B: At., Mol. Opt. Phys. **36**, 1041 (2003).

[43] D. Leibfried, R. Blatt, C. Monroe, and D. Wineland, Quantum dynamics of single trapped ions, Rev. Mod. Phys. **75**, 281 (2003).

[44] J. Johansson, P. Nation, and F. Nori, QuTiP 2: A Python framework for the dynamics of open quantum systems, Comput. Phys. Commun. **184**, 1234 (2013).

[45] C. Cohen-Tannoudji, J. Dupont-Roc, and G. Grynberg, Atom–photon interactions: Basic processes and applications (1993).

[46] S. Zippilliand and G. Morigi, Mechanical effects of optical resonators on driven trapped atoms: Ground-state cooling in a high-finesse cavity, Phys. Rev. A **72**, 053408 (2005).